Quantum Manipulation of Trapped Ions in Two Dimensional Coulomb Crystals.

D. Porras[1,*] and J. I. Cirac[1,†]

[1] *Max-Planck-Institut für Quantenoptik, Hans-Kopfermann-Str. 1, Garching, D-85748, Germany.*

(Dated: February 19, 2008)

We show that a large number of ions stored in a Penning trap, and forming a 2D Coulomb crystal, provides an almost ideal system for scalable quantum computation and quantum simulation. In particular, the coupling of the internal states to the motion of the ions transverse to the crystal plane, allows one to implement two qubit quantum gates. We analyze in detail the decoherence induced by anharmonic couplings with in–plane hot vibrational modes, and show that very high gate fidelities can be achieved with current experimental set–ups.

The search for a physical system where quantum computation is feasible is at the focus of an intense theoretical and experimental activity [1]. Ion traps are by now among the most promising candidates for a many–qubit quantum processor. In this system, qubits are stored in internal electronic states, and collective vibrational modes of the ions allow us to induce quantum gates between them [2]. Following this idea, the building blocks for quantum computation have already been demonstrated in experiments with a few qubits [3]. Most of the current efforts to scale up the size of current ion quantum processors, rely on the fabrication of arrays of microtraps [4], in which a large number of ions can be stored and shuttled. Even though an astonishing progress has been achieved in this direction in the last years, the scalability of this system still demands technical advances in microfabrication and trap design [5].

Penning traps provide us with an alternative trapping scheme, where a large number of ions (10^4 – 10^6) can be confined by a potential with approximate cylindrical symmetry [6]. Axial confinement is induced by a static electric field, whereas radial confinement is a result of the rotation of the ions under an axial magnetic field. If the axial confinement is strong enough, ions arrange themselves in a triangular lattice on a single plane, which corresponds to a classical two dimensional (2D) Wigner crystal. The appeal of this system lies on the fact that ions are naturally ordered in a 2D regular array, without the need of individual micropotentials. Furthermore, ions are separated by distances of the order of tens of microns, such that they are individually addressable by optical means [7]. Thus, ions in Penning traps may appear as ideally suited for quantum computation and quantum simulation. However, this system has never been considered for this task [8]. First, because the complicated vibrational level structure of the 2D crystal makes it difficult to apply here schemes that require resolution of single vibrational modes. Beside that, typical schemes usually rely on the coupling of qubits to modes in directions parallel to the crystal. In current experiments with Penning traps, Doppler cooling of ions has reached temperatures of at most 1 mK, which implies occupation numbers of 10^2 – 10^3 in the in–plane vibrational modes, so that, it seems not to be possible to use them for quantum operations.

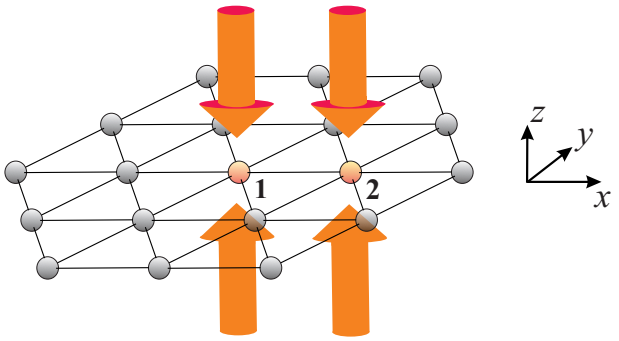

FIG. 1: (color online). Quantum gate in a 2D Coulomb crystal: standing–waves induce a state-dependent dipole force on two nearest neighbors in a triangular lattice.

In this Letter we show how to circumvent these problems by exploiting the ions' motion along the *axial* direction (Fig. 1). This approach benefits from the high axial confinement frequencies (and thus smaller occupation numbers at finite temperature), as well as from the fact that ions are weakly coupled in this direction, something that enormously simplifies the description of the ions' motion. In particular, we show how it is possible to carry out two-qubit gates between ions with high fidelities by performing a careful analysis of the main sources of decoherence. We emphasize that the results derived here also imply that this system is ideally suited for quantum simulations, which may be specially interesting due to the fact that ions are displayed in a triangular structure and favor the simulation of magnetic frustrated systems.

The main source of decoherence in our scheme is due to the anharmonic terms in the Coulomb interaction, which induce a coupling between axial motion and in–plane hot vibrational modes, and lead to a residual qubit–phonon coupling. The description of such decoherence poses an involved theoretical problem, because of the large number of vibrational modes that participate in the process.

*Electronic address: Diego.Porras@mpq.mpg.de
†Electronic address: Ignacio.Cirac@mpq.mpg.de

However, it gets simplified due to the fact that the environment is in a gaussian state, which allows us to simplify the calculation of correlation functions that appear in finite–temperature, time–dependent perturbation theory. We show that in a range of parameters where axial confinement is large enough, the error induced in the quantum gate is very small. Furthermore, the adjustment of the gate time allows us to correct for the influence of the phonon environment, and decrease the gate error by more than one order of magnitude.

Let us consider a system of N ions forming a 2D Coulomb crystal in a Penning trap. We study, for concreteness, the performance of a "pushing gate" [9] in the axial direction, an approach that has the advantage that single vibrational modes do not have to be resolved, and the gate can operate at finite temperature. Since we are interested in estimating the consequences of decoherence, we can neglect finite size effects, and describe the crystal by a regular triangular lattice with periodic boundary conditions. Let us assign the $\mathbf{z}$ direction to the axis of the trap, such that ions occupy equilibrium positions in the $\mathbf{x}$–$\mathbf{y}$ plane:

$$\mathbf{R}^0_{\mathbf{r}} = (r_1\mathbf{a}_1 + r_2\mathbf{a}_2)d_0, \quad r_j = 1, \ldots, L, \tag{1}$$

where $\mathbf{a}_1 = (1, 0, 0)$, $\mathbf{a}_2 = (1/2, \sqrt{3}/2, 0)$, and d_0 is the distance between ions. The potential is given by a trapping term, plus the Coulomb repulsion:

$$\begin{aligned} V &= V_{\rm Trap} + V_{\rm Coul}, \\ V_{\rm Coul} &= \frac{1}{2}\sum_{\mathbf{r},\mathbf{s}} \frac{e^2}{|\mathbf{R}^0_{\mathbf{r}} - \mathbf{R}^0_{\mathbf{s}} + \mathbf{R}_{\mathbf{r}} - \mathbf{R}_{\mathbf{s}}|}. \end{aligned} \tag{2}$$

$\mathbf{R}_{\mathbf{r}} = (X_{\mathbf{r}}, Y_{\mathbf{r}}, Z_{\mathbf{r}})$, are the ions' coordinates with respect to the equilibrium positions, and $V_{\rm Trap}$ is the harmonic trapping potential, with frequencies ω_j in each spatial direction, $j = x, y, z$. Note that in a Penning trap, (2) corresponds to the potential in a frame rotating with the ion crystal [10].

In the harmonic approximation, $V_{\rm Coul}$ is expanded up to second order in $\mathbf{R}_{\mathbf{r}}$, and the axial ($\mathbf{z}$) and in–plane ($\mathbf{x}, \mathbf{y}$) modes are independent. The vibrational harmonic Hamiltonian is given by:

$$H^{(0)}_{\rm vib} = \sum_{\lambda,\mathbf{q}} \hbar\omega^\lambda_{\mathbf{q}} a^\dagger_{\mathbf{q},\lambda} a_{\mathbf{q},\lambda}. \tag{3}$$

$\mathbf{q}$ is the phonon wave–vector, and λ runs over the three possible polarizations: $\lambda = z$ (axial modes), and the two in–plane modes ($\lambda = \parallel, \perp$) corresponding to longitudinal and transverse modes. Local displacements can be expressed in terms of collective coordinates:

$$\begin{aligned} \mathbf{R}_{\mathbf{r}} &= (1/\sqrt{N}) \sum_{\lambda,\mathbf{q}} \mathbf{e}^\lambda_{\mathbf{q}} R^\lambda_{\mathbf{q}} e^{i\mathbf{qr}}, \\ R^\lambda_{\mathbf{q}} &= \sqrt{\hbar/2m\omega^\lambda_{\mathbf{q}}} \left(a^\dagger_{\mathbf{q}} + a_{-\mathbf{q}}\right). \end{aligned} \tag{4}$$

where $\mathbf{e}^\lambda_{\mathbf{q}}$ are the polarization vectors, which are eigenstates of the Fourier transform of the harmonic ion–ion interaction [11]:

$$\begin{aligned} \Omega^{i,j}_{\mathbf{q}} &= \delta_{i,j}\, \omega_j^2 + \sum_{\mathbf{s}} \frac{e^2}{m}(1 - \cos(\mathbf{sq}))V^{i,j}_{\mathbf{s}}, \\ V^{i,j}_{\mathbf{s}} &= \frac{1}{|\mathbf{R}^0_{\mathbf{s}}|^3}\left(\frac{3(\mathbf{R}^0_{\mathbf{s}})_i(\mathbf{R}^0_{\mathbf{s}})_j}{|\mathbf{R}^0_{\mathbf{s}}|^2} - \delta_{i,j}\right). \end{aligned} \tag{5}$$

For each $\mathbf{q}$, $\omega^\lambda_{\mathbf{q}}$ are given by the eigenvectors of the 3×3 matrix $\sqrt{\Omega_{\mathbf{q}}}$.

The "pushing gate" works by coupling the internal states of two ions, which we label 1 and 2, to the axial ($\mathbf{z}$) motion [9, 12]. An off–resonant standing–wave induces a force which displaces the position of ions 1 and 2, in a direction which depends on their internal state [13] (Fig. 1):

$$H_{\rm f}(t) = \sum_{j=1,2} F(t) Z_{\mathbf{r}_j} \sigma^z_j, \tag{6}$$

where σ^z_j are operators acting on the internal states of ions at sites $\mathbf{r}_j$. To simplify our calculations, we consider the following time–dependent force: $F(t) = Fe^{-i\Gamma|t|/2}$ ($-\infty < t < \infty$). However, our results are qualitatively valid for other pulse shapes with gate time $1/\Gamma$. Trapping parameters are chosen such that $\beta_z = e^2/m\omega_z^2 d_0^3 \ll 1$ [13]. In this limit, ions moving in the axial direction can be considered as independent harmonic oscillators weakly coupled by the Coulomb interaction, akin to the case of microtrap arrays. Furthermore, we will be in the adiabatic limit, defined here by:

$$\mathcal{E}_z = 8(\Gamma/\omega_z)^2 (FZ_0/\hbar\omega_z)^2 (2\bar{n}_z + 1) \ll 1, \tag{7}$$

where Z_0 is the axial ground state size, and $\bar{n}_z$ is the mean axial phonon number. $\mathcal{E}_z$ is, indeed, the error induced in the quantum gate by nonadiabatic effects in the axial vibrational degrees of freedom [12]. Under condition (7), internal states end up being decoupled from the axial motion after the gate, and follow the unitary evolution given by:

$$U_{\rm g} = e^{-i\int dt J(t)\sigma^z_1\sigma^z_2}, \; J(t) = 2\beta_z \left(\frac{F(t)Z_0}{\hbar\omega_z}\right)^2 \omega_z. \tag{8}$$

In the following we consider the choice $\Gamma = J(0)\pi/8$, such that $U_{\rm g}$ corresponds, up to local operations, to a sign gate.

Unfortunately, the axial motion is coupled to the in–plane modes by anharmonic terms in $V_{\rm Coul}$, being the lowest order ones of the form XZ^2, X^2Z^2, that is, quadratic in the axial coordinates. Since resonances between axial and in–plane vibrational frequencies lead to divergences in the correlation functions of these terms, the effect of anharmonicities is reduced if $\omega^z_{\mathbf{q}} \gg 2\,\omega^{\parallel,\perp}_{\mathbf{q}}$. The axial vibrational bandwidth is proportional to β_z, and, thus, this condition can be imposed by choosing a thight enough axial confinement (see [14]). In the case of $N = 10^4$ ions, $\omega_z \approx 50\,\omega_{\rm xy}$ is enough to ensure this

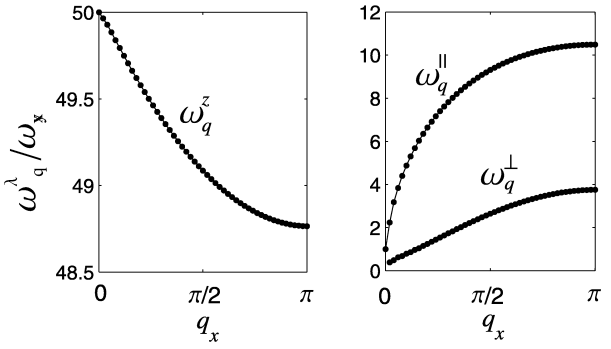

FIG. 2: Spectrum of the vibrational modes with wavevector $\mathbf{q}$ along the $\mathbf{x}$ direction. $N = 10^4$ ions, $\omega_z = 50\omega_{\rm xy}$, and we consider periodic boundary conditions.

condition (see Fig. 2), so that we will assume this ratio in all the examples presented along this work.

Let us now quantify the loss of fidelity induced by anharmonic couplings. The force (6) displaces the ions in the axial direction by $\bar{Z}(t) = 2F(t)Z_0^2/\hbar\omega_z$. In the limit (7), ions 1 and 2 follow adiabatically the displacement induced by the force, so that one can neglect the fluctuations in the coordinates $Z_{\mathbf{r}_j}$, and replace them by their ground state average, $\bar{Z}(t)\sigma_j^z$, when computing anharmonic corrections. The anharmonic energy dependence on the ions' position results in the following coupling between internal states and in–plane modes:

$$\begin{aligned} H_{\rm xy}^{\rm dec}(t) &= H_{\rm xy}^{\rm ah}(t)\frac{1}{4}\left(\sigma_1^z-\sigma_2^z\right)^2, \\ H_{\rm xy}^{\rm ah}(t) &= \bar{Z}(t)^2\left(\mathbf{A}^{\rm T}\ \mathbf{R}_{1,2}\ +\mathbf{R}_{1,2}^{\rm T}\mathbf{B}\ \mathbf{R}_{1,2}\right). \end{aligned} \quad (9)$$

$\mathbf{R}_{1,2}$ ($\mathbf{R}_{1,2}^0$) is the vector given by the in–plane components of $\mathbf{R}_{\mathbf{r}_1}-\mathbf{R}_{\mathbf{r}_2}$ ($\mathbf{R}_{\mathbf{r}_1}^0-\mathbf{R}_{\mathbf{r}_2}^0$). $\mathbf{A}$ and $\mathbf{B}$ are third and fourth order anharmonic Coulomb interaction terms, respectively:

$$\mathbf{A} = 3\frac{e^2}{d_0^5}\mathbf{R}_{1,2}^0, \quad \mathbf{B} = \frac{3e^2}{d_0^5}\left(\mathbf{1}-\frac{5}{2}\frac{\mathbf{R}_{1,2}^0\ (\mathbf{R}_{1,2}^0)^{\rm T}}{d_0^2}\right). \quad (10)$$

Note that $H_{\rm xy}^{\rm dec}$ excites the in–plane phonons depending on the ions' internal states, and, thus, entangles the qubits with the environment.

Assume that the internal states are initially in a pure state: $|\Psi\rangle = \sum_\alpha c_\alpha|\alpha\rangle$ ($|\alpha\rangle = |00\rangle, |01\rangle, |10\rangle, |11\rangle$), such that the initial density matrix of the total system is given by: $\rho_i = |\Psi\rangle\langle\Psi| \otimes \rho_{\rm xy}^0$, with $\rho_{\rm xy}^0$, a thermal phonon state. After the action of the quantum gate, the final density matrix is:

$$\rho_f = \sum_{\alpha,\beta} c_\alpha c_\beta^* \left(U_{\rm g}|\alpha\rangle\langle\beta|U_{\rm g}^\dagger\right)\left(U_{\rm xy}^\alpha\rho_{\rm xy}^0(U_{\rm xy}^\beta)^\dagger\right), \quad (11)$$

where $U_{\rm xy}^\alpha$, is the evolution operator of the in–plane phonons, $U_{\rm xy}$, projected in the internal state α. In (11) we have assumed that the axial modes can be described classically in $H_{\rm xy}^{\rm dec}$ due to the adiabaticity of the quantum gate, such that we can factorize the evolution operator. We define the (worst–case) reduced fidelity, $\mathcal{F}$, of the quantum gate by the overlap of the qubits' reduced density matrix obtained from (11), with the qubit quantum state after a perfect gate, minimized over all possible two–qubit initial states. Note that $U_{\rm xy}^{00} = U_{\rm xy}^{11} = U_{\rm xy}^{[0]}$, and $U_{\rm xy}^{01} = U_{\rm xy}^{10} = U_{\rm xy}^{[\rm ah]}$, where $U_{\rm xy}^{[0]}$ and $U_{\rm xy}^{[\rm ah]}$, are the in–plane phonon evolution operator in the absence and presence of anharmonic couplings, respectively. Thus, the fidelity is completely determined by the following complex quantity $\bar{\mathcal{F}}$:

$$\begin{aligned} \bar{\mathcal{F}} &= {\rm tr}\left\{|01\rangle\langle 00|\rho_i\right\} = {\rm tr}_{\rm xy}\left\{U_{\rm xy}^{[\rm ah]}\rho_{\rm xy}^0 U_{\rm xy}^{[0]\dagger}\right\} \\ &= {\rm tr}_{\rm xy}\left\{\mathcal{T}\exp\left(-i\int_{-\infty}^{\infty}H_{\rm xy}^{\rm ah}(\tau)d\tau\right)\ \rho_{\rm xy}^0\right\}, \end{aligned} \quad (12)$$

which corresponds to the mean value of the evolution operator $U_{\rm xy}^{[\rm ah]}$, in the interaction picture with respect to $H_{\rm xy}^{\rm ah}$. Note that (12) is similar to the expression found in the theory developed in [16]. The worst–case error is $\mathcal{E} = 1-\mathcal{F} = (1-\Re(\bar{\mathcal{F}}))/2$. However, note that the fidelity can be improved, since, according to Eq. (9), the spin–phonon coupling depends on the operator $(1-\sigma_1^z\sigma_2^z)$. For this reason, a correction of the gate time allows us to cancel the phase of $\bar{\mathcal{F}}$, and define $\mathcal{E}' = (1-|\bar{\mathcal{F}}|)/2$, which quantifies the worst–case error after the correct calibration of the gate duration.

Eq. (12) is a good starting point for perturbation theory, which can be carried out by expanding the time–ordered exponential. First of all, let us study the scaling of the terms appearing in $H_{\rm xy}^{\rm ah}$, and check whether a peturbative approach is indeed justified. The anharmonic coupling (9) can be rewritten in terms of collective variables in the interaction picture:

$$H_{\rm xy}^{\rm ah}(\tau) = \sum_{\lambda,\mathbf{q}} F_{\mathbf{q}}^\lambda(\tau)R_{\mathbf{q}}^\lambda(\tau) + \sum_{\lambda,\lambda',\mathbf{q},\mathbf{k}} G_{\mathbf{qk}}^{\lambda\lambda'}(\tau)R_{\mathbf{q}}^\lambda(\tau)R_{\mathbf{k}}^{\lambda'}(\tau), \quad (13)$$

According to Eqs. (8, 9, 10), each term scales like:

$$\begin{aligned} \overline{F_{\mathbf{q}}^\lambda R_{\mathbf{q}}^\lambda} &\approx J\frac{X_0}{d_0} \approx \Gamma\left(\frac{X_0}{d_0}\right), \\ \overline{G_{\mathbf{q},\mathbf{k}}^{\lambda,\lambda'}R_{\mathbf{q}}^\lambda R_{\mathbf{k}}^{\lambda'}} &\approx J\left(\frac{X_0}{d_0}\right)^2 \approx \Gamma\left(\frac{X_0}{d_0}\right)^2, \end{aligned} \quad (14)$$

where X_0 is the size of the ground state in the radial trapping potential, and by $\overline{O}$, we mean the square root of the variance of the operator in the ground state. Since the evolution of the in–plane modes is governed by the in–plane trapping frequency, $\omega_{\rm xy}$, we expect that terms in perturbation theory scale according to $\Gamma/\omega_{\rm xy}$ in Eq. (14). We study two sets of experimental parameters with $\omega_{\rm xy} =$ 20 (200) kHz, and $\omega_z = 1$ (10) MHz, which implies $d_0 =$ 46.8 (10.1) μm. Let us consider $N = 10^4$ ions, such that both values lead to $\beta_z = 3.8\cdot 10^{-3}$. Typical temperatures

of $T = 1$ mK can be reached after Doppler cooling, such that mean phonon numbers are $\bar{n}_z \approx 20$ (2) in the axial modes, and $\bar{n}_{\rm xy} \approx 10^3$ (10^2), in the center of mass in–plane modes. If we choose $(FZ_0/\hbar\omega_z) = 0.234$, such that $\mathcal{E}_z < 10^{-5}$, we get $\Gamma/\omega_{\rm xy} = 5\ 10^{-2}$. Taking into account that X_0/d_0 is small (as it should be, if the assumption of harmonic vibrational modes is valid), all terms are small in (14). In particular, $X_0/d_0 = 3.6 \cdot 10^{-3}$, and $5.0 \cdot 10^{-3}$, in the cases $\omega_{\rm xy} = 20$, and 200 kHz, respectively.

To quantify precisely the error in the quantum gate, we proceed as follows (see the Appendix for the details). We expand the time ordered exponential (12) up to fourth order in $H^{\rm ah}_{\rm xy}$, and keep all the terms up to order $(X_0/d_0)^4$. Each contribution can be expressed in terms of time integrations of correlation functions of collective coordinates $R^\lambda_{\mathbf{q}}$. Resonances appear, for example, in those terms of second order in $G^{\lambda,\lambda'}_{\mathbf{q},\mathbf{k}}$ which are of the form $\langle R^\lambda_{\mathbf{q}}(t_1) R^{\lambda'}_{\mathbf{k}}(t_1) R^\lambda_{-\mathbf{q}}(t_2) R^{\lambda'}_{-\mathbf{k}}(t_2)\rangle$ The problem gets numerically tractable by the application of Wick's theorem, which allows us to express real time high order correlation functions in terms of the two–operator correlation function. Note that Wick's theorem can be applied here, even when we are at finite temperatures, because of the statistical properties of the phonon thermal (gaussian) state. Finally, a summation of sets of diagrams up to infinite order is possible by means of the linked cluster theorem, such that (12) takes finally the form of the exponential of low order irreducible diagrams [17].

The results of our calculation are presented in Fig. 3, where we show our results for the two sets of experimental parameters discussed above. Note that at high temperatures, like those ones that occur in current experiments with Penning traps, we get a quadratic dependence with temperature, which can be explained by the dominant contribution of terms that are second order in the coupling $G^{\lambda,\lambda'}_{\mathbf{q},\mathbf{k}}$. The correction of the phase by adjustment of the gate time allows us to reduce the error by more than one order of magnitude. Note that even with the highest temperatures considered here, which correspond to the limit of Doppler cooling, anharmonic terms induce very small errors. With the range of parameters considered in this work, we get rates $\Gamma = 1$, 10 kHz. A limitation in the number of quantum gates due to heating, reduces the number of gates to a maximum of $\approx 10^2$, with present heating rates, however, this quantity is amenable to be improved by increasing the quality of the vacuum in the trap [18] .

Finally, our proposal could also be used for the quantum simulation of interacting spin–systems, by applying a state dependent force to all the ions at the same time. In this way, as shown in Ref. [19], an antiferromagnetic Ising interaction is induced between the internal states, which behave like effective spins. If we add a transverse field of the form $(\Omega/2)\sum_{\mathbf{r}} \sigma^x_{\mathbf{r}}$, by means of a global carrier transition, then this experimental set–up allows us to study the rich phenomenology of quantum frustration in triangular lattices [20]. Note that our analysis of the decoherence induced by low–energy vibrational modes, also implies the viability of this approach, since the effective spin–spin interactions are an always–on version of the qubit–qubit coupling induced during the quantum gate.

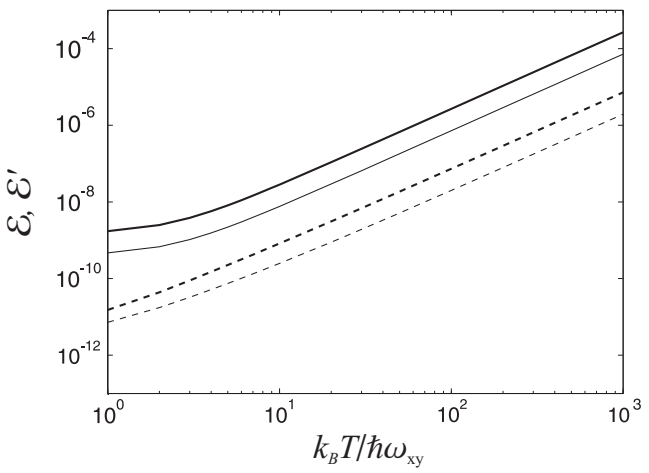

FIG. 3: Continuous lines: $\mathcal{E}$ (error without phase correction). Dashed lines: $\mathcal{E}'$ (error with correction of the gate time. Thick lines and thin lines, correspond to $\omega_{\rm xy} = 20$ kHz and $\omega_{\rm xy} = 200$ kHz, respectively. $N = 10^4$ ions and $\Gamma/\omega_{\rm xy} = 0.05$.

We thank J. Bollinger, D. Leibfried and M. Aguado for interesting discussions. Work supported by CONQUEST, SCALA, and Marie Curie under contract MEIF–2004–010350.

APPENDIX A: PROPERTIES OF A WIGNER 2D CRYSTAL

(In this appendix, we describe in more detail the properties of a 2D Wigner crystal, as well as the calculation of the decoherence in the quantum gate due to coupling with low–energy vibrational modes. For the sake of readability, we repeat a few of the equations already presented in the main text.)

We express the potential in the rotating frame in terms of the equilibrium positions $\mathbf{R}^0_{\mathbf{r}}$, and the coordinates of the ions with respect to the equilibrium positons, $\mathbf{R}_{\mathbf{r}}$:

$$
\begin{aligned}
V &= V_{\rm Coul} + V_{\rm Trap}, \\
V_{\rm Coul} &= \frac{1}{2}\sum_{\mathbf{r},\mathbf{s}} \frac{e^2}{|\mathbf{R}^0_{\mathbf{r}} - \mathbf{R}^0_{\mathbf{s}} + \mathbf{R}_{\mathbf{r}} - \mathbf{R}_{\mathbf{s}}|}, \\
V_{\rm Trap} &= \frac{1}{2} m\omega_z^2 \sum_{\mathbf{r}} \left(Z^0_{\mathbf{r}} + Z_{\mathbf{r}}\right)^2 + \\
&+ \frac{1}{2} m\omega_r^2 \sum_{\mathbf{r}} \left(\left(X^0_{\mathbf{r}} + X_{\mathbf{r}}\right)^2 + \left(Y^0_{\mathbf{r}} + Y_{\mathbf{r}}\right)^2 \right). \qquad \text{(A1)}
\end{aligned}
$$

In the case $\omega_z \gg \omega_{\rm xy}$, the Coulomb crystal is a single plane, which corresponds to a 2D Wigner crystal. Under

these conditions, ions arrange themselves in the triangular lattice generated by (1).

The theoretical description of this system becomes much simpler if we consider periodic boundary conditions, something that is a good approximation, since we deal with large number of particles. The equilibrium positions in a 2D Wigner crystal are given by a triangular lattice generated by:

$$\mathbf{a}_1 = (1, 0, 0), \qquad \mathbf{a}_2 = (1/2, \sqrt{3}/2, 0). \tag{A2}$$

The reciprocal lattice is generated by the following vectors:

$$\mathbf{b}_1 = (1, -1/\sqrt{3}, 0), \qquad \mathbf{b}_2 = (0, 2/\sqrt{3}, 0), \tag{A3}$$

The basis of the reciprocal lattice is determined by the relations: $(\mathbf{a})_i \cdot (\mathbf{b})_j = \delta_{i,j}$. They are the allowed directions of propagation given by the periodicity of the ion lattice.

Since we are considering a lattice with regular spacing, we can easily determine the ions' equilibrium positions. In this simple case, this task is reduced to finding the equilibrium distance between ions, d_0, which we prefer to express in terms of the adimensional parameter $\beta_{\rm xy}$:

$$\begin{aligned} \beta_{\rm xy}(L) &= \frac{2e^2}{m\omega_{\rm xy}^2 d_0^3} = \frac{4C_1(L)}{L^2 C_2(L)}, \\ C_1(L) &= \sum_{\mathbf{s}} |\mathbf{R}_{\mathbf{s}}^0|^2, \\ C_2(L) &= \sum_{\mathbf{s}} 1/|\mathbf{R}_{\mathbf{s}}^0|. \end{aligned} \tag{A4}$$

To determine dynamical properties of the Coulomb crystal, we study now the normal vibrational modes, which diagonalize the motion Hamiltonian in the harmonic approximation. Remember that these ones are given by plane–waves of the following form:

$$\begin{aligned} \mathbf{R}_{\mathbf{q}} &= \frac{1}{L} \sum_{\mathbf{r}} e^{i\mathbf{q}\mathbf{r}} \mathbf{R}_{\mathbf{r}}, \\ \mathbf{P}_{\mathbf{p}} &= \frac{1}{L} \sum_{\mathbf{r}} e^{-i\mathbf{p}\mathbf{r}} \mathbf{P}_{\mathbf{r}}. \end{aligned} \tag{A5}$$

Let us keep in mind that these are not hermitian operators $(\mathbf{R}_{\mathbf{q}})^\dagger = \mathbf{R}_{-\mathbf{q}}$. They satisfy the commutation relations: $[\mathbf{R}_{\mathbf{q}}^i, \mathbf{P}_{\mathbf{p}}^j] = i\delta_{\mathbf{q},\mathbf{p}}\delta_{i,j}$, such that the harmonic Hamiltonian is finally written like this:

$$H_{vib}^{(0)} = \sum_{\mathbf{q},i,j} \frac{1}{2} m \Omega_{\mathbf{q}}^{i,j} (\mathbf{R}_{\mathbf{q}})^i (\mathbf{R}_{-\mathbf{q}})^j + \sum_{\mathbf{q}} \frac{1}{2m} \mathbf{P}_{\mathbf{q}} \mathbf{P}_{-\mathbf{q}}. \tag{A6}$$

Where the dispersion relation is the Fourier transform of the relative potential, see Eq. (5). Allowed phonon wavevectors are $\mathbf{q} = q_1\mathbf{b}_1 + q_2\mathbf{b}_2$, that is, it is a vector of the reciprocal lattice (otherwise the plane–waves do not satisfy the orthogonality relations on the triangular lattice). Local coordinates can be finally written like:

$$\begin{aligned} \mathbf{R}_{\mathbf{r}} &= \frac{1}{L} \sum_{\lambda,\mathbf{q}} e^{-i\mathbf{q}\mathbf{r}} \mathbf{e}_{\mathbf{q}}^{\lambda} \sqrt{\frac{\hbar}{2m\omega_{\mathbf{q}}^{\lambda}}} \left(a_{\lambda,\mathbf{q}}^\dagger + a_{\lambda,-\mathbf{q}} \right), \\ \mathbf{P}_{\mathbf{r}} &= \frac{i}{L} \sum_{\lambda,\mathbf{q}} e^{-i\mathbf{q}\mathbf{r}} \mathbf{e}_{\mathbf{q}}^{\lambda} \sqrt{\frac{m\hbar\omega_{\mathbf{q}}^{\lambda}}{2}} \left(a_{\lambda,\mathbf{q}}^\dagger - a_{\lambda,-\mathbf{q}} \right), \end{aligned} \tag{A7}$$

where $\mathbf{e}_{\mathbf{q}}^{\lambda}$ determine the direction of vibration of the mode, and the index λ can take three values which correspond to longitudinal or transverse modes in the in–plane direction, and vibration perpendicular to the Coulomb crystal plane.

The anharmonic corrections to the vibrational Hamiltonian that are relevant for us, are those which couple the axial ($\mathbf{z}$) to the in–plane motion ($\mathbf{x}$, $\mathbf{y}$), because they will lead eventually to the qubit–phonon couplings presented in Eq. (9). Let us writte them explicitly:

$$\begin{aligned} H_{\rm ah} &= \frac{1}{2} \sum_{\substack{\mathbf{r},\mathbf{s} \\ i=x,y}} A_{\mathbf{r},\mathbf{s}}^i \, (\mathbf{R}_{\mathbf{r},\mathbf{s}})^i (\mathbf{R}_{\mathbf{r},\mathbf{s}})^z + \\ &+ \frac{1}{2} \sum_{\substack{\mathbf{r},\mathbf{s} \\ i,j=x,y}} B_{\mathbf{r},\mathbf{s}}^{i,j} \, (\mathbf{R}_{\mathbf{r},\mathbf{s}})^i (\mathbf{R}_{\mathbf{r},\mathbf{s}})^j (\mathbf{R}_{\mathbf{r},\mathbf{s}})^z. \end{aligned} \tag{A8}$$

where $\mathbf{R}_{\mathbf{r},\mathbf{s}} = \mathbf{R}_{\mathbf{r}} - \mathbf{R}_{\mathbf{s}}$. Note that we include in $H_{\rm ah}$ only those terms that have the form $H_{\rm ah} \approx X\ Z^2 + X^2\ Z^2$. The anharmonic coupling constants given by:

$$\begin{aligned} A_{\mathbf{r},\mathbf{s}}^i &= \frac{3}{4} \frac{e^2}{d_0^5} \frac{\left(\mathbf{R}_{\mathbf{r},\mathbf{s}}^0\right)^i}{|\mathbf{R}_{\mathbf{r},\mathbf{s}}^0|^4}, \\ B_{\mathbf{r},\mathbf{s}}^{i,j} &= \frac{3}{8} \frac{e^2}{d_0^5} \left(2\delta_{i,j} - 5 \frac{\left(\mathbf{R}_{\mathbf{r},\mathbf{s}}^0\right)^i \left(\mathbf{R}_{\mathbf{r},\mathbf{s}}^0\right)^j}{|\mathbf{R}_{\mathbf{r},\mathbf{s}}^0|^5}, \right). \end{aligned} \tag{A9}$$

Again, we define relative coordinates $\mathbf{R}_{\mathbf{r},\mathbf{s}}^0 = \mathbf{R}_{\mathbf{r}}^0 - \mathbf{R}_{\mathbf{s}}^0$.

Since we want to induce a quantum gate between ions by means of an internal–state dependent force in the axial ($\mathbf{z}$) direction, the position of the ions will depend, in the adiabatic limit of the gate, on the internal state. This induces a coupling between qubits and in–plane modes, through the dependence of (A8) on $\mathbf{R}^z$. To get an explicit form for this coupling, let us first introduce the formalism for describing a pushing gate between to nearest–neigbors in the Coulomb crystal.

APPENDIX B: PUSHING GATE IN THE AXIAL DIRECTION

Our goal now is to study the performance of the pushing gate under the presence of anharmonic terms. First of all, let us collect all the terms that describe our system:

$$\begin{aligned} H(t) &= H_0(t) + H_{\rm ah}, \\ H_0(t) &= H_{\rm vib}^{(0)} + H_{\rm f}(t) \end{aligned} \tag{B1}$$

$H_0(t)$ is the harmonic part of the Hamiltonian, and can be solved exactly. We include in it the vibrational Hamiltonian:

$$H_{\rm vib}^{(0)} = \sum_{\lambda,\mathbf{q}} \hbar\omega_{\lambda,\mathbf{q}} a^\dagger_{\lambda,\mathbf{q}} a_{\lambda,\mathbf{q}}, \tag{B2}$$

as well as the force in the axial direction:

$$H_{\rm f} = \sum_{j=1,2} F(t) Z_{\mathbf{r}_j} \sigma_j^z. \tag{B3}$$

Under the set of conditions considered in this work, the error in the quantum gate is the sum of two independent contributions: *(i)* nonadiabatic effects due to the excitation of phonons in the axial direction (common to any implementation of the pushing gate), and *(ii)* the errors induced by anharmonic couplings. Our strategy will be, first, to solve $H_0(t)$, then to study $H_{\rm ah}$ in the interaction picture with respect to $H_0(t)$, and finally to evaluate the effect of the anharmonic couplings by doing perturbation theory.

For later convenience, we choose the following temporal profile for the amplitude of the off–resonant standing wave:

$$F(t)^2 = F^2 P(t), \qquad P(t) = e^{-\Gamma|t|}. \tag{B4}$$

We define an interaction picture with respect to $H_{\rm ah}$, which has the only unusual feature that $H_0(t)$ is time–dependent:

$$\begin{aligned} U_{\rm I}(t) &= U_0^\dagger(t) U(t), \\ \partial_t U_{\rm I}(t) &= -\frac{i}{\hbar} U_0^\dagger(t) H_{\rm ah} U_0(t), \end{aligned} \tag{B5}$$

where $U(t)$, $U_0(t)$, are the evolution operators corresponding to $H(t)$, $H_0(t)$, respectively, and $U_{\rm I}(t)$ is the evolution operator in the interaction picture.

We consider the limit $\beta_z \ll 1$, that is, the Coulomb interaction between ions is small with respect to the trapping potentials. The problem could be easily extended to the general case, but remember that this condition has to be fulfilled to avoid crossings between in–plane modes and the axial motion of the ions. In this limit, the evolution operator consists of qubit–qubit couplings, as well as the displacement induced by the force (which can be considered independently for each ion):

$$\begin{aligned} U_0(t) &= U_{\rm g}(t) e^{-iH_{\rm vib}^{(0)} t} e^{\sum_{j=1,2}\left(\eta(t)^* a_{z,j} - \eta(t) a^\dagger_{z,j}\right)\sigma_j^z}, \\ U_{\rm g}(t) &= e^{-i\int_{-\infty}^{t} J(\tau)\sigma_1^z\sigma_2^z d\tau}, \end{aligned} \tag{B6}$$

where $\eta(t)$ determines the time–dependent displacement of each ion's position:

$$\eta^*(t) = (-i)\int_{-\infty}^{t} \frac{F(\tau) Z_0}{\hbar} e^{-i\omega_z\tau} d\tau, \tag{B7}$$

Furthermore, we consider the adiabatic limit, $\Gamma \ll \omega_z$, in which the coupling $J(t)$ is given by:

$$J(t) = 2\beta_z \left(\frac{F(t) Z_0}{\hbar\omega_z}\right)^2 \hbar\omega_z, \tag{B8}$$

and the ions 1 and 2 are displaced by the state-dependent force in the following way:

$$U_0^\dagger(t) Z_j U_0(t) = Z_j(t) + 2\eta(t) Z_0 \sigma_j^z \tag{B9}$$

with $\eta(t)$ given by:

$$\eta(t) = \frac{F(t) Z_0}{\hbar\omega_z} \tag{B10}$$

The coupling of the qubits with the in–plane vibrational modes is obtained formally by studying the evolution of $H_{\rm ah}$ in the interaction picture:

$$\begin{aligned} H_{\rm ah}^{\rm I}(t) &= U_0^\dagger(t) H_{\rm ah} U_0(t) \approx \\ -4\eta(t)^2 Z_0^2 &\left((\sigma_1^{\rm z} - \sigma_2^{\rm z})^2 A^i_{\mathbf{r}_1,\mathbf{r}_2} \sum_i (\mathbf{R}_{\mathbf{r}_1,\mathbf{r}_2})^i + \right. \\ &\left. \sum_{i,j} B^{i,j}_{\mathbf{r}_1,\mathbf{r}_2} \, (\mathbf{R}_{\mathbf{r}_1,\mathbf{r}_2})^i (\mathbf{R}_{\mathbf{r}_1,\mathbf{r}_2})^j \right) = H_{\rm xy}^{\rm dec}(t). \end{aligned} \tag{B11}$$

In the last equation we have neglected all the terms that depend on the operators Z_j, because they give negligible contributions in the adiabatic limit of the quantum gate. In this limit, Eq. (B11) reduces to a coupling between in–plane vibrational modes and qubits, which does not involve any quantum dynamics in the axial motion. Recall that Eq. (B11) defines $H_{\rm xy}^{\rm dec}$, that is, the coupling that we have used in the main text.

We have already stated the problem in terms that are suitable to study the fidelity of the pushing gate. For this task, let us assume that the internal states are initially in a pure state:

$$|\Psi\rangle = \sum_\alpha c_\alpha |\alpha\rangle, \quad |\alpha\rangle = |00\rangle, |01\rangle, |10\rangle, |11\rangle. \tag{B12}$$

In this appendix we are describing both the error induced by in–plane modes, and the error due to nonadiabatic corrections in the axial motion, so that we study the density matrix of the whole system (axial modes, in–plane modes, and qubits). Let us consider, an initial density matrix for the system, which describes the initial qubit pure state, and thermal phonon states $\rho_{\rm z}^0$, $\rho_{\rm xy}^0$:

$$\rho_i = |\Psi\rangle\langle\Psi| \otimes \rho_{\rm z}^0 \otimes \rho_{\rm xy}^0 \tag{B13}$$

After the action of the quantum gate, the final density matrix is:

$$\rho_f = \sum_{\alpha,\beta} c_\alpha c_\beta^* \left(U_{\rm g}|\alpha\rangle\langle\beta|U_{\rm g}^\dagger\right) \left(U_{\rm z}^\alpha \rho_{\rm z}^0 (U_{\rm z}^\beta)^\dagger\right) \left(U_{\rm xy}^\alpha \rho_{\rm xy}^0 (U_{\rm xy}^\beta)^\dagger\right). \tag{B14}$$

In Eq. (B14), $U_{\rm z}^\alpha$, $U_{\rm xy}^\alpha$, are the unitary evolution of the vibrational modes in directions $\mathbf{z}$, and $\mathbf{x}$–$\mathbf{y}$, respectively, proyected into the qubits' quantum state α, that is:

$$\begin{aligned} U_{\rm z}^\alpha(t) &= e^{\sum_{j=1,2}\left(\eta(t)^* a_{z,j} - \eta(t) a^\dagger_{z,j}\right)\langle\alpha|\sigma_j^z|\alpha\rangle} e^{-iH_{\rm z}^0 t}, \\ U_{\rm xy}^\alpha(t) &= e^{-iH_{\rm xy}^0 t} \mathcal{T} \exp\left(\int_{-\infty}^{t} \langle\alpha|H_{\rm ah}^{\rm I}(\tau)|\alpha\rangle d\tau\right). \end{aligned} \tag{B15}$$

where we have used the time–ordered exponential $\mathcal{T}\exp$, to express the evolution operator in the interaction picture with respect to $H_{\rm ah}$. We define $\mathcal{F}$, the reduced fidelity, as the overlap of the qubits' reduced fidelity obtained from ρ_f, with a pure qubit–state after the action of the unitary operation, $U_{\rm g}$:

$$\mathcal{F} = \sum_{\alpha,\beta} |c_\alpha|^2 |c_\beta|^2 \mathcal{F}_{\rm z}^{\alpha,\beta} \mathcal{F}_{\rm xy}^{\alpha,\beta} \tag{B16}$$

where we have defined the following quantities:

$$\begin{aligned} \mathcal{F}_{\rm z}^{\alpha,\beta} &= {\rm tr}_{\rm z}\left(U_{\rm z}^{\alpha}\rho_{\rm z}^0 (U_{\rm z}^{\beta})^\dagger\right), \\ \mathcal{F}_{\rm xy}^{\alpha,\beta} &= {\rm tr}_{\rm xy}\left(U_{\rm xy}^{\alpha}\rho_{\rm xy}^0 (U_{\rm xy}^{\beta})^\dagger\right). \end{aligned} \tag{B17}$$

$\mathcal{F}_{\rm z}$ includes the decoherence induced in the quantum gate by the finite gate rate, Γ, something that is general to any quantum gate that relies on the adiabatic displacement of vibrational modes (see, for example, [12]). Its value can be easily evaluated:

$$\mathcal{F}_{\rm z}^{\alpha,\beta} = e^{-|\eta_{\rm ND}|^2(\bar{n}_z+1/2)\left((\langle\sigma_1^z\rangle_\alpha - \langle\sigma_1^z\rangle_\beta)^2 + (\langle\sigma_2^z\rangle_\alpha - \langle\sigma_2^z\rangle_\beta)^2\right)}. \tag{B18}$$

where $\eta_{\rm ND}$ includes the corrections due to nonadiabaticity, namely:

$$\eta_{ND} = -2i\frac{FZ_0}{\hbar\omega_z}\frac{\Gamma}{\omega_z}. \tag{B19}$$

where Z_0 is the ground state size in the axial trapping potential. The contribution to the error can be estimated from (B18). For this, we consider that we are in the limit of small errors, and minimize $\mathcal{F}_{\rm z}$ with respect to all the possible initial states, to get the worst–case error, which is given by:

$$\mathcal{E}^z \approx 4\eta^2(\bar{n}+1/2) \approx 16\left(\frac{\Gamma}{\omega_z}\right)^2\left(\frac{FZ_0}{\omega_z}\right)^2. \tag{B20}$$

The main point of this work is the calculation of the decoherence that is inherent to this system, that is, the one induced by the coupling of the qubits to the in–plane motion. Since this one poses a more complicated problem, we will be dedicated to it during the next sections to it

APPENDIX C: DECOHERENCE INDUCED BY COUPLING TO IN–PLANE VIBRATIONAL MODES

Let us see how to express $\mathcal{F}_{\rm xy}$ in a form that is suitable for doing perturbation theory in the anharmonic couplings. First of all, note that the only matrix elements $\langle\alpha|H_{\rm ah}^I|\alpha\rangle$ which are different from zero are those with $|\alpha\rangle = |01\rangle, |10\rangle$:

$$H_{\rm xy}^{\rm ah} = \langle\alpha|H_{\rm xy}^{\rm dec}|\alpha\rangle \tag{C1}$$

The only quantity that we have to evaluate to calculate the contribution to $\mathcal{F}$ in (B17) is the following one:

$$\bar{\mathcal{F}}_{\rm xy} = {\rm tr}_{\rm xy}\left(\mathcal{T}\exp\left(\int_{-\infty}^{t} H_{\rm xy}^{\rm ah}(\tau)d\tau\right)\right) \tag{C2}$$

Note that $\bar{\mathcal{F}}_{\rm xy}$ is named simply as $\bar{\mathcal{F}}$ in the main text, because we focus there on the decoherence induced by coupling to x–y vibrational modes only.

We assume that the ion 1 is at the position $\mathbf{R}_{\mathbf{r}_1}^0 = (0,0)$, and 2 is at $\mathbf{R}^0\mathbf{r}_2 = (1,0)$, so that the following substitution allows us to express the coupling terms as a function of normal modes:

$$(\mathbf{R}_{\mathbf{r}_1})^i - (\mathbf{R}_{\mathbf{r}_2})^i = \frac{1}{L}\sum_{\mathbf{q},\lambda}\left(\mathbf{e}_{\mathbf{q}}^{\lambda}\right)^i (1-e^{iq_1})R_{\mathbf{q}}^{\lambda} \tag{C3}$$

We rewrite here $H_{\rm xy}^{\rm ah}$ in a form that is more suitable to study the scaling of the error with the different parameters of the problem:

$$\begin{aligned} H_{\rm xy}^{\rm ah}(\tau) &= \bar{F}P(\tau)\frac{1}{L}\sum_{\lambda,\mathbf{q}} F_{\mathbf{q}}^{\lambda}\tilde{R}_{\mathbf{q}}^{\lambda}(\tau) + \\ &\quad \frac{1}{L^2}\bar{G}P(\tau)\sum_{\mathbf{q},\mathbf{k},\lambda,\lambda'} G_{\mathbf{q},\mathbf{k}}^{\lambda,\lambda'}\tilde{R}_{\mathbf{q}}^{\lambda}(\tau)\tilde{R}_{\mathbf{k}}^{\lambda'}(\tau), \\ F_{\mathbf{q}}^{\lambda} &= \mathbf{e}_{q,\lambda}^{x}(1-e^{iq_x}), \\ G_{\mathbf{q},\mathbf{k}}^{\lambda,\lambda'} &= \sum_{i,j}(2\delta_{i,j} - 5\delta_{i,x}\delta_{j,x}) \\ &\quad \mathbf{e}_{\mathbf{q},\lambda}^{i}\mathbf{e}_{\mathbf{k},\lambda'}^{j}(1-e^{iq_x})(1-e^{ik_x}). \end{aligned} \tag{C4}$$

We define: $\eta(t)^2 = \eta^2 P(t)$, where $P(t)$ is defined in Eq. (B4), and $\eta = \eta(0) = FZ_0/\hbar\omega_z$. In (C4), we have defined the adimensional coordinates:

$$\tilde{R}_{\mathbf{k}}^{\lambda} = R_{\mathbf{k}}^{\lambda}/X_0 \tag{C5}$$

where we have defined the ground state size in the radial trapping potential, $X_0 = \sqrt{\hbar/(2m\omega_r)}$. The spin–phonon coupling constants are:

$$\begin{aligned} \bar{F} &= -16\eta^2\bar{z}^2 X_0\frac{3e^2}{4d_0^4} = -6\beta_z\eta^2\omega_z\left(\frac{X_0}{d_0}\right), \\ \bar{G} &= -16\eta^2\bar{z}^2(X_0)^2\frac{3}{8}\frac{e^2}{d_0^5} = -3\beta_z\eta^2\omega_z\left(\frac{X_0}{d_0}\right)^2. \end{aligned} \tag{C6}$$

The advantage of expression (C6) is that it shows explicitly the scaling of the coupling of the qubits with the in–plane vibrational modes in terms of the relevant quantities of the problem.

In the Taylor expansion of (C2), only time–ordered terms appear. Even when we are at finite–temperature, Wick's theorem applies [17], something that can be shown by means of the path integral formalism, or by studying directly the generating functional of the correlation functions (see the last section of this appendix). In this way, one can express every term in perturbation theory as integrations of the contractions of the theory,

which we define here in the following way:

$$D^{\lambda,\lambda'}_{\mathbf{q},-\mathbf{k}}(1,2) = D^{\lambda,\lambda'}_{\mathbf{q},-\mathbf{k}}(t_1 - t_2),$$
$$D^{\lambda,\lambda'}_{\mathbf{q},-\mathbf{k}}(\tau) = \langle \mathcal{T}\{\tilde{R}^{\lambda}_{\mathbf{q}}(\tau)\tilde{R}^{\lambda'}_{-\mathbf{k}}(0)\}\rangle$$
$$= \frac{\omega_{\rm xy}}{\omega^{\lambda}_{\mathbf{q}}}\Big(n_{\mathbf{q},\lambda}e^{i\omega_{\mathbf{q}}\tau} + n_{\mathbf{q},\lambda}e^{-i\omega^{\lambda}_{\mathbf{q}}\tau} + \theta(\tau)e^{-i\omega^{\lambda}_{\mathbf{q}}\tau} + \theta(-\tau)e^{i\omega_{\lambda,\mathbf{q}}\tau}\Big)\delta_{\mathbf{q},-\mathbf{k}}\delta_{\lambda,\lambda'}. \quad \text{(C7)}$$

where we made explicit that in the limit of high temperatures time–order does not matter and our task should be infinitely simplified.

When calculating terms in perturbation theory,

$$D^{\lambda,\lambda}_{\mathbf{q},-\mathbf{q}}(\tau) = \frac{1}{2\pi}\int_{-\infty}^{\infty} e^{i\omega\tau}D^{\lambda,\lambda}_{\mathbf{q},-\mathbf{q}}(\omega)d\omega. \quad \text{(C8)}$$

We will make use the following identity:

$$e^{i\omega^{\lambda}_{\mathbf{q}}\tau}\theta(\pm\tau) = \frac{\pm 1}{2\pi i}\int_{-\infty}^{\infty}\frac{e^{i\omega\tau}}{\omega - \omega^{\lambda}_{\mathbf{q}} \mp i\delta}d\omega. \quad \text{(C9)}$$

So that:

$$D^{\lambda,\lambda}_{\mathbf{q},-\mathbf{q}}(\omega) = \frac{\omega_{\rm xy}}{\omega^{\lambda}_{\mathbf{q}}}\Big(n_{\lambda,\mathbf{q}}2\pi\delta(\omega - \omega^{\lambda}_{\mathbf{q}}) + n_{\lambda,\mathbf{q}}2\pi\delta(\omega + \omega^{\lambda}_{\mathbf{q}}) + \frac{2i\omega^{\lambda}_{\mathbf{q}}}{\omega^2 - (\omega^{\lambda}_{\mathbf{q}})^2 + i\delta}\Big) \quad \text{(C10)}$$

The reader is going to find out the reason for our choice of exponential pulses: their Fourier transform is a Lorentzian, which is better suited for integrations with the phonon propagator in Eq. (C10),

$$P(t) = \frac{1}{2\pi}\int d\omega e^{i\omega t}P(\omega),$$
$$P(\omega) = \frac{2\Gamma}{\omega^2 + \Gamma^2}. \quad \text{(C11)}$$

The energy scales of this problem are J, Γ, ω_r, and T. J and Γ are related by the requirement that a sign gate is realized by the coupling to the axial modes, that is $J = \frac{\pi}{8}\Gamma$, something that allows us to rewrite the coupling constants in a self–consitent way:

$$\bar{F} = -\frac{3}{4}\pi\left(\frac{X_0}{d_0}\right)\Gamma,$$
$$\bar{G} = -\frac{3}{8}\pi\left(\frac{X_0}{d_0}\right)^2\Gamma. \quad \text{(C12)}$$

Thus, it is clear from the previous expression, that $\bar{F}$, $\bar{G}$ are small, both if $X_0/d_0 \ll 1$, and in the case in which the quantum gate is also adiabatic with respect to the in–plane motion. However, the scaling of the coupling constants with these parameters does not allows us to extract definitive conclusions about the decoherence, because the energies of the vibrational modes are strongly corrected by the Coulomb energy (see Fig. 2).

APPENDIX D: PERTURBATION THEORY

In this section, we present the calculation of the contributions to the expansion of $\mathcal{F}_{\rm xy}$ which are of fourth order in (X_0/d_0), that is, up to $\mathcal{O}(\bar{F}^4)$, $\mathcal{O}(\bar{G}^2)$, $\mathcal{O}(\bar{G}\bar{F}^2)$.

We have to evaluate time ordered averages of products of operators of the form:

$$\langle \mathcal{T}\{R^{\lambda_1}_{\mathbf{k}_1}(t_1)\dots R^{\lambda_n}_{\mathbf{k}_n}(t_n)\}\rangle. \quad \text{(D1)}$$

The average $\langle\rangle$ is understood as a thermal average over the in–plane vibrational modes. The calculation of time ordered correlation functions becomes simplified by the use of Wick's theorem. Even when it is usually stated in terms of an operator identity that is useful only at zero temperature, Wick's theorem can be applied to finite temperature, by using the fact that a thermal state is gaussian, and thus correlation functions can be obtained as functional derivatives of a gaussian functional. We give more details of this point in the following subsection. For the moment, let us recall that Wick's theorem states that (D1) can be expressed as a sum of products of two–time correlation functions, each of them corresponding to a possible pairing of the operators:

$$\langle \mathcal{T}\{R^{\lambda_1}_{\mathbf{k}_1}(t_1)\dots R^{\lambda_n}_{\mathbf{k}_n}(t_n)\}\rangle =$$
$$D^{\lambda_1,\lambda_2}_{\mathbf{k}_1,\mathbf{k}_2}(t_1–t_2)D^{\lambda_3,\lambda_4}_{\mathbf{k}_3,\mathbf{k}_4}(t_3–t_4)\dots D^{\lambda_{n-1},\lambda_n}_{\mathbf{k}_{n-1},\mathbf{k}_n}(t_{n-1}–t_n) +$$
$$D^{\lambda_1,\lambda_3}_{\mathbf{k}_1,\mathbf{k}_3}(t_1–t_3)D^{\lambda_2,\lambda_4}_{\mathbf{k}_2,\mathbf{k}_4}(t_2–t_4)\dots D^{\lambda_{n-1},\lambda_n}_{\mathbf{k}_{n-1},\mathbf{k}_n}(t_{n-1}–t_n) +$$
$$\dots \text{(all possible pairings)}. \quad \text{(D2)}$$

Note that Wick's theorem allows us to apply the cluster theorem to the expansion of the time order exponential in Eq. (C2), that is:

$$\bar{\mathcal{F}}_{\rm xy} = \exp\left(\mathcal{E}^{(1)} + \mathcal{E}^{(2)} + \dots\right), \quad \text{(D3)}$$

where $\mathcal{E}^{(n)}$ are disconnected contributions only, that is, terms in which the time integrations cannot be factorized into separate independent time integrations.

1. First order in $H^{\rm ah}_{\rm xy}$

The lowest order contribution is given by:

$$\mathcal{E}^{(1)} = (-i)\frac{\bar{G}}{L^2}\sum_{\mathbf{k},\lambda}G^{\lambda,\lambda}_{\mathbf{k},-\mathbf{k}}\int_{-\infty}^{\infty}dtP(t)\langle\tilde{R}^{\lambda}_{\mathbf{k}}(t)\tilde{R}^{\lambda}_{-\mathbf{k}}(t)\rangle$$
$$= (-i)\frac{2\bar{G}}{\Gamma}\frac{1}{L^2}\sum_{\mathbf{k},\lambda}G^{\lambda,\lambda}_{\mathbf{k},-\mathbf{k}}\bar{x}^2_{\lambda,\mathbf{k}}(2n_{\lambda,\mathbf{k}} + 1). \quad \text{(D4)}$$

where we used $\bar{x}_{\lambda,\mathbf{k}} = 1/\sqrt{\omega^{\lambda}_{\mathbf{k}}/\omega_{\rm xy}}$, and $n_{\lambda,\mathbf{k}}$ is the occupation number of the mode with polarization λ, and wave–vector $\mathbf{k}$. Note that this is purely imaginary, thus it should not contribute to the error, after a correction of the gate time.

2. Second order in $H_{\rm xy}^{\rm ah}$

We find two connected terms:

$$\mathcal{E}^{(2)} = -\frac{1}{2L}\bar{F}^2\sum_{\mathbf{q},\lambda}F^{\lambda}_{\mathbf{q}}F^{\lambda}_{-\mathbf{q}} \int P(t_1)D^{\lambda,\lambda}_{\mathbf{q},-\mathbf{q}}(t_1-t_2)P(t_2)dt_1dt_2. \quad \text{(D5)}$$

We solve the integration in frequency space:

$$\int P(t_1)P(t_2)D^{\lambda,\lambda}_{\mathbf{q},-\mathbf{q}}(t_1-t_2)dt_1dt_2 = \int \frac{d\omega}{2\pi}P(\omega)^2 D^{\lambda,\lambda}_{\mathbf{q},-\mathbf{q}}(\omega) = (2n_{\lambda,\mathbf{q}}+1)\bar{x}^2_{\lambda,\mathbf{q}}\frac{(2\Gamma)^2}{(\Gamma^2+(\omega^{\lambda}_{\mathbf{q}})^2)^2} -2i\bar{x}^2_{\lambda,\mathbf{q}}\left(\frac{\omega^{\lambda}_{\mathbf{q}}}{\Gamma}\frac{1}{\Gamma^2+(\omega^{\lambda}_{\mathbf{q}})^2}+\frac{2\omega^{\lambda}_{\mathbf{q}}\Gamma}{(\Gamma^2+(\omega^{\lambda}_{\mathbf{q}})^2)^2}\right). \quad \text{(D6)}$$

Since $(\bar{F}/\Gamma)\approx X_0/d_0$, it is convenient to rewrite this expression in the following form. The second disconnected contribution of order two in $H_{\rm xy}^{\rm ah}$, is:

$$\mathcal{E}^{(3)} = -\frac{1}{L^4}\bar{G}^2\sum_{\mathbf{q},\mathbf{k},\lambda,\lambda'}G^{\lambda,\lambda'}_{\mathbf{q},\mathbf{k}}G^{\lambda,\lambda'}_{-\mathbf{q},-\mathbf{k}} \int\frac{d\omega d\omega'}{(2\pi)^2}P(\omega+\omega')^2 D^{\lambda,\lambda}_{\mathbf{q},-\mathbf{q}}(\omega)D^{\lambda',\lambda'}_{\mathbf{k},-\mathbf{k}}(\omega'). \quad \text{(D7)}$$

The integrations are easily solved in the complex plane by contour integration, however, the resulting expressions are cumbersome, and bring very little to the discussion of the results. The limit of high temperatures, which is valid for most of the temperature range considered in Fig. 3, is more easily handled:

$$\mathcal{E}^{(3)} = -\frac{1}{L^4}\bar{G}^2\sum_{\mathbf{q},\mathbf{k},\lambda,\lambda'}G^{\lambda,\lambda'}_{\mathbf{q},\mathbf{k}}G^{\lambda,\lambda'}_{-\mathbf{q},-\mathbf{k}} n_{\lambda,\mathbf{q}}n_{\lambda',\mathbf{k}}\left(2P(\omega^{\lambda}_{\mathbf{q}}+\omega^{\lambda'}_{\mathbf{k}})+2P(\omega^{\lambda}_{\mathbf{q}}-\omega^{\lambda'}_{\mathbf{k}})\right). \quad \text{(D8)}$$

Note that $P(\omega^{\lambda}_{\mathbf{q}}-\omega^{\lambda'}_{\mathbf{k}})$ contain terms that will diverge in the limit $\Gamma\to 0$, so that, their numerical evaluation is necesary for a quantitative understanding of the dissipation during the quantum gate.

3. Third order in $H_{\rm xy}^{\rm ah}$

The only disconnected contribution is given by:

$$\mathcal{E}^{(4)} = i\frac{1}{L^4}\bar{F}^2\bar{G}\sum_{\substack{\lambda,\lambda'\\ \mathbf{q},\mathbf{k}}}F^{\lambda}_{-\mathbf{q}}F^{\lambda'}_{-\mathbf{k}}G^{\lambda,\lambda'}_{\mathbf{q},\mathbf{k}}\times \int\frac{d\omega d\omega'}{(2\pi)^2}P(\omega)P(\omega')P(\omega+\omega')D^{\lambda,\lambda}_{\mathbf{q},-\mathbf{q}}(\omega)D^{\lambda',\lambda'}_{\mathbf{k},-\mathbf{k}}(\omega'). \quad \text{(D9)}$$

Again, we writte here explicitly the result for high temperatures, that is:

$$\mathcal{E}^{(4)} = i\frac{1}{L^4}\bar{F}^2\bar{G}\sum_{\substack{\lambda,\lambda'\\ \mathbf{q},\mathbf{k}}}F^{\lambda}_{-\mathbf{q}}F^{\lambda'}_{-\mathbf{k}}G^{\lambda,\lambda'}_{\mathbf{q},\mathbf{k}}n_{\lambda,\mathbf{q}}n_{\lambda',\mathbf{k}}\times 2P(\omega^{\lambda}_{\mathbf{q}})P(\omega^{\lambda'}_{\mathbf{k}})\left(P(\omega^{\lambda}_{\mathbf{q}}+\omega^{\lambda'}_{\mathbf{k}})+P(\omega^{\lambda}_{\mathbf{q}}-\omega^{\lambda'}_{\mathbf{k}})\right) \quad \text{(D10)}$$

Where we find, again, a divergence due to resonant terms in the limit $\Gamma\to 0$.

APPENDIX E: SHORT NOTE ABOUT THE WICK'S THEOREM AT FINITE TEMPERATURE

Since it seems that there is some confussion in the literature about the validity of this approach, we show here that Wick's theorem can be justified at finite temperatures.

Let us define the generating functional, which functional derivation yields the time ordered correlation functions:

$$\langle\mathcal{T}\{R_{\mathbf{k}_1}(t_1)\dots R_{\mathbf{k}_n}(t_n)\}\rangle = \frac{\delta}{i\delta j_{\mathbf{k}_1}(t_1)}\cdots\frac{\delta}{i\delta j_{\mathbf{k}_n}(t_n)}\frac{1}{\mathcal{Z}_0}\mathcal{Z}[j(x)], \quad \mathcal{Z}=\mathrm{tr}\{e^{-\beta H_0}\mathcal{T}e^{i\sum_{\mathbf{k}}\int_{-\infty}^{\infty}j_{\mathbf{k}}(t)X_{\mathbf{k}}(t)dt}\}. \quad \text{(E1)}$$

This could be the starting point for defining a path integral representation, but it is much easier to calculate explicitly the time–ordered exponential. First of all a small detail: it is convenient to consider $j_{\mathbf{k}}(x)$ as belonging to the set of continuous functions that satisfy $j_{-\mathbf{k}}(x)=j^*_{\mathbf{k}}(x)$, so that the exponent is anti–hermitian. Note that the generating functional (E1) has the same form as the evolution operator of a forced harmonic oscillator, thus, its form can be explicitly obtained, by following the same lines. In any case, since the conmutators of the exponents at different times, are itself quadratic forms of the currents $j_{\mathbf{k}}$, it is clear that the generating functional is gaussian. Since its second functional derivative yields the time ordered correlation function of tow position operators, the only choice is the following one:

$$\mathcal{Z}[j(x)]/\mathcal{Z}_{\prime} = \exp\sum_{\mathbf{k}}\left(+\frac{1}{2}\int_{-\infty}^{\infty}j_{-\mathbf{k}}(t_1)D_{\mathbf{k}}(t_1-t_2)j_{\mathbf{k}}(t_2)\,dt_1dt_2\right) \quad \text{(E2)}$$

where the kernel of the functional, $D_{\mathbf{k}}(t_1-t_2)$, is the correlation function defined in the previous sections. Higher order functional differentiation leads immediately to Wick's theorem.

APPENDIX F: EFFECTIVE SPIN–SPIN INTERACTIONS INDUCED BY A WALKING–WAVE

Finally, we introduce here a scheme for inducing effective spin-spin interactions which relies on the use of a walking wave. This is a different approach to the one presented in [19], which relies on the coupling of the internal states of the ions to the motion by means of a standing wave. The latter approach might be difficult to implement, since one needs to fix the position of the ions relative to the minima of the standing wave. This condition is not necesary in the walking wave scheme, something that may be useful in quantum simulations with ions in Paul or Penning traps.

A walking wave, like the one used by the NIST group for the geometrical phase gate [3], leads to a spin–motion coupling of the following form:

$$H_{\rm f} = \frac{\Omega}{2}\left(e^{ik(x_0+x_j)-i\omega_L t} + e^{-ik(x_0+x_j)+i\omega_L t}\right)\sigma_j^z, \quad \text{(F1)}$$

where ω_L is the detuning of the laser beams that create the walking wave. We consider that $\mathbf{x}$ is a direction transverse to the Coulomb crystal, that is, the radial direction in the case of a linear chain, or the axial direction in a 2D Coulomb crystal. If the walking wave propagates in this direction, then all the ions are at the same position, x_0 with respect to the walking wave. Note also that we are neglecting ac Stark shifts, which can be cancelled in a laser configuration like the one used at NIST [3].

We consider here that the vibrational modes of the ions are in the "stiff" limit, that is, the trapping potential is much larger the Coulomb repulsion between ions. The validity of this limit can be quantified by means of the following quantity:

$$\beta_x \equiv \frac{e^2}{m d_0^3 \omega_x^2}, \quad \text{(F2)}$$

where d_0 is the mean distance between ions. If $\beta_x \ll 1$, then the energy of the vibrational modes is not strongly modified by the Coulomb interaction, and all the modes are close in energy. Indeed, β_x is an approximation to the dispersion in the energies of the vibrational modes, ω_n. Let us say that ω_x is the trapping frequency. Then, all the energies lie below ω_x, and satisfy that:

$$(1-\beta_x)\,\omega_x \lesssim \omega_n < \omega_x. \quad \text{(F3)}$$

If we consider the Lamb–Dicke expansion of (F1), then:

$$\begin{aligned} H_{\rm f}(t) &\approx \frac{\Omega}{2}\left(e^{ikx_0-i\omega_L t} + h.c.\right)\sigma^z \\ &+ \frac{\Omega}{2}\left(ike^{ikx_0}e^{-i\omega_L t}\sum_j x_j + h.c.\right)\sigma_j^z. \quad \text{(F4)} \end{aligned}$$

Our idea is the following: in the case $\beta_x \ll 1$, one can tune ω_L to the red–sideband with respect to all the vibrational frequencies in (F4) (see Fig. 4), because in this case, ions are close to be independent. In the end, this will lead to a coupling of the form $\sum_j x_j\sigma_j^z$, which will induce an effective spin–spin interaction just in the same way as in our previous proposals, with the advantage that the amplitude of the force does not depend now on the position of the ions relative to the phase of the walking wave.

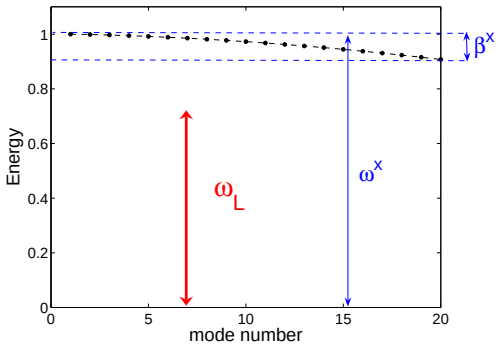

FIG. 4: Radial vibrational normal modes of a chain with 20 ions, and ration between radial and trapping frequencies: $\omega_r/\omega_z = 10$.

Let us describe this situation formally. First, remember that the position of the ions can be expressed in terms of normal modes:

$$x_j = \sum_n \mathcal{M}_{j,n}\left(\frac{\hbar}{2m\omega_n}\right)^{1/2}\left(a_n + a_n^\dagger\right). \quad \text{(F5)}$$

where $\mathcal{M}$ are matrices that diagonalize the harmonic motion of the ions (they are basically sines and cosines).

We want to tune ω_L to the red sideband with respect to all the modes ω_n, so that we choose $\omega_L < \omega_n$, and $\omega_x - \omega_n \ll \omega_n$. Under these conditions we can keep only the red sideband terms of (F4):

$$\begin{aligned} H_{\rm f}(t) &\approx \sum_n \left(g_n^* a_n e^{i\omega_L t} + g_n a_n^\dagger e^{-i\omega_L t}\right), \\ g_n &= \sum_j ik\frac{\Omega}{2}e^{ikx_0}\left(\frac{\hbar}{2m\omega_n}\right)^{1/2}\mathcal{M}_{j,n}\,\sigma_j^z. \quad \text{(F6)} \end{aligned}$$

The rotation of the terms in (F6) can be eliminated by considering the phonons in a rotating frame, in which their energy is shifted by ω_L. The whole hamiltonian in this frame reads:

$$\begin{aligned} H &= H_0 + H_{\rm f}(0) \\ &= \sum_n \hbar\delta_n a_n^\dagger a_n + \sum_n \left(g_n^* a_n + g_n a_n^\dagger\right), \quad \text{(F7)} \end{aligned}$$

with $\delta_n = \omega_n - \omega_L$. Note that (F7) induces a state dependent force on all the ions simultaneously. A difference with the pushing gate approach is that vibrational energies suffer a shift that we can controll by tuning ω_L.

To deal with this coupling we use, as usual, a canonical transformation, to map our system to a quantum spin model:

$$\begin{aligned} \mathcal{S} &= \sum_n \left(\eta_n^* a_n - \eta_n a_n^\dagger\right) \\ \eta_n &\equiv \frac{g_n}{\hbar\delta_n}. \end{aligned} \tag{F8}$$

Under this transformation, the internal states of the ions follow the dynamics of a spin–spin Hamiltonian:

$$H \to e^{-\mathcal{S}} H e^{\mathcal{S}} = H_0 + \frac{1}{2} J_{j,k} \sum_{j,k} \sigma_j^z \sigma_k^z. \tag{F9}$$

The effective spin–spin interaction is given by:

$$J_{j,k} \equiv \sum_n \frac{|F^2|}{m\omega_n \delta_n} \mathcal{M}_{j,n} \mathcal{M}_{k,n}. \tag{F10}$$

where is the force induced by the walking wave, $F = ik(\Omega/2)e^{-ikx_0}$. The spin–spin interaction does not depend on the absolute position of the ion crystal, or the ion plane.

Note that one important difference with our previous work is that now the shifted frequencies appear in the denominator, thus, we can expect that the dependence of $J_{j,k}$ on the inter–ion distance will be different, and even suitable to be controlled by tuning ω_L.

Let us now estimate the strength of $J_{j,k}$ in the simplest case. For this, let us recall that the normal vibrational modes can be written like this:

$$(\omega_n)^2 = (\omega_x)^2 \left(1 + \beta_x V_n\right), \tag{F11}$$

where V_n is the contribution from the Coulomb interaction. So to say, V_n contains the dispersion of the modes in Fig. 4. V_n can be obtained from the harmonic terms of the Coulomb interaction by means of the transformation defined by the matrices $\mathcal{M}$:

$$\sum_n \mathcal{M}_{j,n} V_n \mathcal{M}_{k,n} = \frac{1}{|j-k|^3}. \tag{F12}$$

On the other hand, the shifted modes fulfill that:

$$\delta_n = (\omega_x)\left(1 + \beta_x V_n\right)^{1/2} - \omega_L. \tag{F13}$$

If these two conditions are met:

$$\beta_x \ll 1, \tag{F14}$$

$$\beta_x \omega_x/(\omega_x - \omega_l) \ll 1, \tag{F15}$$

then we can express ω_n and δ_n in a series in β_x, and get the following approximate relation for the effective interaction:

$$\begin{aligned} J_{j,k} &\approx \beta_x \frac{1}{2} \frac{|F|^2}{m(\omega_x - \omega_L)^2} \frac{1}{|j-k|^3} = \\ &= \beta_x \left(\frac{F x_0}{\omega_x - \omega_L}\right)^2 \frac{1}{|j-k|^3}\, \omega_x, \end{aligned} \tag{F16}$$

where we have also used that $\omega_x - \omega_L \ll \omega_x$, and x_0 is the ground state size in the trapping potential. Note that condition $\beta_x \ll 1$ has to hold if we want to be able to resolve the red sideband simultaneously for all the vibrational modes, but condition (F15), on the contrary, can be avoided, the only difference being that the effective spin-spin interaction will deviate from the $1/r^3$ decay in Eq. (F16).

The expression (F10) does not tell us much about the interaction rate that can be achieved in an experiment. For this, one has to take into account the error that is introduced in the simulation by the coupling of the qubits (effective spins) to the vibrational modes.

We have already studied in detail this error (see [19]), which depends on the displacement of the modes. The error in the quantum simulation is induced by the entanglement of the vibrational modes with the effective spins, and it can be approximated by the following quantity:

$$\mathcal{E} \approx \eta^2 = \frac{|F x_0|^2}{\hbar(\omega_x - \omega_L)}, \tag{F17}$$

which is simply an approximation to the coefficients η_n in Eq. (F8). The strength of the effective interaction is $J \approx \beta_x \eta^2 \omega_x$. Thus, we find the same relation that in the case of the standing wave.

Last, one has to take into account the effect of the first term in Eq. (F4). Even in the limit $\Omega/\omega_L \ll 1$, one could get into troubles in case that corrections of the form Ω^2/ω_L appear. We will see that this is not the case, because this term is diagonal in σ^z. It can be rewritten in the following way:

$$\begin{aligned} H_{\rm c} &= \epsilon(t)\sigma^z, \\ \epsilon(t) &= \Omega \cos(k x_0 - \omega_L t), \end{aligned} \tag{F18}$$

such that the eigenstates are the same, with time evolution given by:

$$\begin{aligned} |\Psi(t)\rangle &= c_\uparrow(t)|\uparrow\rangle + c_\downarrow(t)|\downarrow\rangle, \\ c_\uparrow(t) &= e^{-i\int_0^t \epsilon(t')dt'}, \\ c_\uparrow(t) &= e^{-i(\Omega/\omega_L)\left(\sin(kx_0^j - \omega_L t) - \sin(kx_0^j)\right)}. \end{aligned} \tag{F19}$$

Thus, the effect of H_c affects terms of the form $B\sigma^x$, and operators $\sigma^\dagger$, get corrections of order $B\Omega/\omega_L$. This means, that condition $\Omega/\omega_l \ll 1$ is enough to guarantee that these corrections are small compared to the effective spin-spin Hamiltonian interaction strengths.

[1] J.I. Cirac and P. Zoller, Phys. Today **57**, 38 (2004).

[2] J. I. Cirac and P. Zoller, Phys. Rev. Lett. **74**, 4091 (1995).

[3] C. Monroe *et al.*, Phys. Rev. Lett. **75**, 4714 (1995); D. Leibfried *et al.*, Nature **422**, 412 (2003); F. Schmidt-Kaler *et al.*, Nature **422**, 408 (2003).

[4] D. Kielpinksi, C. Monroe, and D.J. Wineland, Nature (London) **417**, 709 (2002); D. Stick *et al.*, Nature Physics **2**, 36 (2006).

[5] T.S. Metodi *et al.*, quant-ph/0509051.

[6] W.M. Itano *et al.*, Science **279**, 686 (1998); T.B. Mitchell *et al.*, Science **282**, 1290 (1998).

[7] T.B. Mitchell *et al.*, Phys. Rev. Lett. **87**, 183001 (2001).

[8] Note that arrays of single electron Penning traps have been proposed for quantum arrays, see G. Ciaramicoli *et al.*, Phys. Rev. Lett. **91**, 017901 (2003).

[9] J.I. Cirac and P. Zoller, Nature **404**, 579 (2000).

[10] We study here the limit in which the cyclotron and rotation frequencies satisfy the relation $\Omega_c/2 = \omega_{\rm md}$, in which there is no magnetic field in the rotating frame.

[11] D.H.E. Dubin, Phys. Rev. Lett. **71**, 2753 (1993).

[12] T. Calarco, J. I. Cirac, and P. Zoller, Phys. Rev. A **63**, 062304 (2001); M. Sasura and A. M. Steane, Phys. Rev. A **67**, 062318 (2003).

[13] The coupling in Eq. (6) can be obtained with a configuration of lasers and polarizations similar to that one presented by Wineland et al. in quant-ph/0212079).

[14] β_z scales like $(\omega_{\rm xy}/\omega_z)^2\sqrt{N}$ [15], thus, it can be tuned by choosing the axial/radial trapping frequency ratio.

[15] D.H.E. Dubin and T.M. O'Neil, Rev. Mod. Phys. **71**, 87 (1999).

[16] M. Znidaric and T. Prozen, J. Phys. A **36**, 2463 (2003) .

[17] J.W. Negele and H. Orland, *Quantum Many–Particle Systems* (Addison–Wesley, New York, 1988).

[18] M.J. Jensen, T. Hasegawa, and J. Bollinger, Phys. Rev. A **70**, 033401 (2004).

[19] D. Porras and J.I. Cirac, Phys. Rev. Lett. **92**, 207901 (2004); X.-L. Deng, D. Porras, and J.I. Cirac, Phys. Rev. A. **72**, 063407 (2005).

[20] G.H. Wannier, Phys. Rev. **79**, 357 (1950); R. Moessner and S.L. Sondhi, Phys. Rev. B **63**, 224401 (2001).